Analysis of the Chandra X-ray Observatory Aspect Camera PSF and its Application to Post-Facto Pointing Aspect Determination

David C. Morris, Thomas L. Aldcroft, Robert A. Cameron, Mark L. Cresitello-Dittmar, Margarita Karovska

Smithsonian Astrophysical Observatory, 60 Garden St., Cambridge, MA, USA

ABSTRACT

For the last 20 months, the Chandra X-Ray Observatory (Weisskopf et. al. 2000) has been producing X-ray images of the universe in stunning detail. This is due in large part to the excellent *post-facto* pointing aspect determination for *Chandra* (Aldcroft et. al. 2000). This aspect determination performance is achieved using elliptical gaussian centroiding techniques. Application of point spread function (PSF) fitting using a true PSF model for the Aspect Camera Assembly (ACA) on *Chandra* could improve this performance. We have investigated the use of an ACA PSF model in the *post-facto* centroiding of stars and fiducial lights imaged by the ACA.

We will present the methodologies explored for use in determining a model for the ACA PSF and discuss the results of a comparison of PSF fit centroiding and the current method of elliptical gaussian centroiding as they apply to *post-facto* aspect reconstruction. The first method of recovering the ACA PSF uses a raytrace model of the ACA to generate simulated stellar PSFs. In this method, the MACOS raytracing software package is used to describe each element of the *Chandra* aspect optical system. The second method investigated is the so called shift and add method whereby we build a high resolution image of the PSF by combining several thousand low resolution images of a single star collected by the ACA while tracking during normal science observations. The programmed dither of the spacecraft slowly sweeps the stellar image across the ACA focal plane, and the many slightly offset images are used to effectively increase the resolution of the resultant image of the star to a fraction of an ACA pixel. In each method, a library of PSF images is built at regularly gridded intervals across the ACA focal plane. This library is then used to interpolate a PSF at any desired position on the focal plane. We have used each method to reprocess the aspect solution of a set of archived *Chandra* observation and compare the results to one another and to the delivered *post-facto* aspect solution, currently derived using elliptical gaussian centroiding of ACA star images. Finally, we will present a summary of *Chandra*'s aspect performance achieved to date, and discuss the effect of incorporating a PSF model into the post-facto aspect determination software.

Keywords: Chandra, Aspect, Raytrace, Point Spread Function, Pointing Performance

1. INTRODUCTION

The Chandra X-ray Observatory was launched aboard the Space Shuttle Columbia on July 23, 1999. Measuring 45 feet long and weighing 50,162 lbs when connected to its IUS at launch, it is the largest payload ever carried aboard a NASA shuttle. The third in NASA's series of Great Observatories, Chandra is designed to greatly exceed the performance of its X-ray predecessors. The half power diameter (HPD) point spread function (PSF) of Chandra's high resolution mirror assembly (HRMA) is $0.5''$, surpassing the HPD of the ROSAT and Einstein missions ($5.0''$) by an order of magnitude and surpassing that of the ASCA mission ($150''$) by more than 2 orders of magnitude. Chandra's X-ray sensitivity is an order of magnitude greater than that of ROSAT.

The Chandra aspect system plays a key role in achieving this X-ray imaging resolution and sensitivity. The science instruments aboard Chandra record the arrival time and position (in detector coordinates) of individual photons. In order to reconstruct a true X-ray image of the sky, an accurate time history of the pointing attitude of the spacecraft is needed. This is made possible with the aspect system, comprising both the on-board Pointing Control and Aspect Determination (PCAD) hardware and the post-facto ground processing software. In order for Chandra to achieve

Further author information: (Send correspondence to David Morris)
David Morris: E-mail: dmorris@head-cfa.harvard.edu

the X-ray resolution and sensitivity noted above, the Chandra aspect system must meet the specifications in Table 1. Also listed in Table 1 are the preflight predicted values and actual flight performance values corresponding to each specification.

The on-board PCAD hardware includes the following sensors, actuators and optics, with associated electronics and support structures:

Aspect Camera Assembly (ACA) 11.2 cm optical telescope, stray light shade, two CCD detectors (primary and redundant) and two sets of electronics. The ACA can track up to 8 images simultaneously. The detectors are 1024x1024 Tektronix CCDs built of 24x24 μm ($5''$ x $5''$) pixels which project to produce a camera field of view of 1.4^o square. The camera's spectral coverage ranges from 4000-9000 angstroms with a sensitivity bias towards the red end of the spectrum. The telescope is deliberately defocused to spread the energy of a single star over several pixels (FWHM $9''$) to allow realtime centroid determination from simple pixel averaging techniques.

Inertial Reference Units (IRU) Two IRUs, each containing two 2-axis, rate-integrating, strapdown gyroscopes. Normal operation has one IRU running, providing data in 4 axes.

Fiducial Light Assemblies (FLA) LEDs mounted around each science instrument (SI) detector which are imaged in the ACA via the fiducial transfer system.

Fiducial Transfer System (FTS) Consists of the retro-reflector collimator (RRC, a corner cube plus collimating lens) mounted at the center of the X-ray optics, and a periscope. The FTS collimates the light from the FLAs and directs it to the ACA, via the retro-reflector and periscope.

Fine Sun Sensor (FSS) A digital sun sensor with a $\pm 50^\circ \times \pm 50^\circ$ field of view and 0.02° resolution.

Coarse Sun Sensor (CSS) Four analog sensors mounted at the outer corners of the *Chandra* solar panels, providing a combined 4π steradian field of view.

Reaction Wheel Assembly (RWA) Six reaction wheels, mounted in a pyramidal configuration. Each RWA can provide 20 in-oz of control torque and 60-ft-lb-sec of momentum storage at bi-directional speeds up to 6000 rpm. Normal operation uses all 6 RWAs.

Momentum Unloading Propulsion System (MUPS) Thrusters used to unload momentum from the RWAs.

Figure 1 shows the layout of the optical components of the PCAD subsystem.

Table 1. Chandra Aspect System performance specifications.

Requirement	Specification	Predicted	Achieved
Absolute Celestial Pointing	$30''$	$17.1''$	$3''$
10 Second RMS Pointing	$0.12''$	$0.05''$	$0.05''$
Image Reconstruction	$0.5''$	$0.34''$	$0.26''$
Celestial Location	$1.0''$	$0.48''$	$0.6''$

The post-facto ground processing software (aspect pipeline) is a collection of tools written in C and C++ which process data from the ACA and IRUs in order to produce a time history of the spacecraft attitude (aspect solution). For each science observation, the aspect processing pipeline software is run as part of the CXC Automatic Processing system. The two most important elements of the aspect pipeline are centroiding the ACA images and combining these centroids with the IRU data via a Kalman filter.

Achieving the necessary accuracy in ACA centroiding ($0.36''$ RMS per axis) is a challenge because of the large ACA pixel scale of $5''$/pixel. This implies centroiding to better than 0.07 pixels. To date, the aspect pipeline has been meeting this requirement by fitting elliptical gaussians to the images. However, an accurate model of the ACA PSF over the field of view could improve pipeline performance in two ways. First, a true model of the PSF would

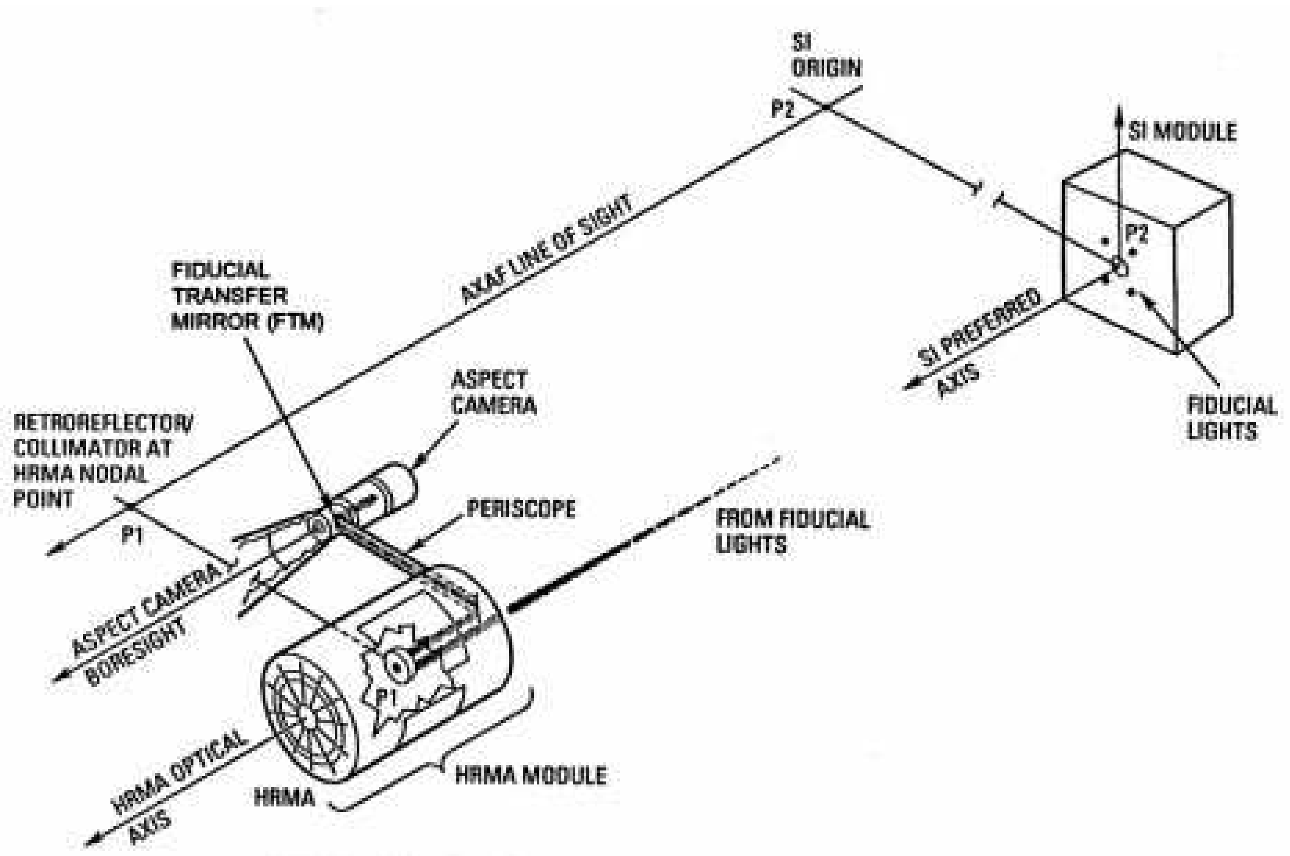

Figure 1. Optical components of the Pointing Control and Aspect Determination subsystem

provide an empirically more accurate method of determining stellar centroids than elliptical gaussian centroiding. Second, PSF fitting of ACA data will allow easier and more accurate identification of ACA pixels with high dark current (hot pixels), which are a primary cause of aspect solution degradation in the current aspect determination software. Hot pixel filtering is currently performed at runtime by the post-facto pipeline by searching for background pixels which exceed a threshold. This technique fails to identify some low level hot pixels though, which may be more easily filtered by PSF fitting.

While PSF calibration data were collected prior to launch using the Better Accuracy Testing System (BATS) at Ball Aerospace, these data cannot precisely reproduce the true structure of the ACA PSF because of the non-pointlike nature of the calibration source. Thus we have investigated two methods of recovering a high resolution model of the ACA PSF: raytracing and super-resolving the ACA image data using a shift and add technique.

2. MODELING DETAILS

2.1. The Raytrace Method

The Raytrace Method used the commercial MACOS and VSIM raytracing software packages, to build a model of the ACA PSF based on information from technical documentation and optical and mechanical construction specifications. The form of the PSF varies significantly over the field of view (fov) of the Aspect Camera as can be seen in Figure 2. Thus we modeled a grid of PSFs spanning the full extent of the ACA focal plane at 90 pixel intervals (a 13x13 grid) across the fov. Each of the 169 PSFs thus produced was modeled with a pixel size of 1/12 the nominal $5''$ ACA pixels ($0.42''$) over 10x10 ACA pixels ($50''$ square).

A 20 element optical prescription was built for the ACA from technical documentation, on the optical elements of the ACA. Because slight changes in optical alignments may have occurred during launch, the elements of the optical prescription were allowed to 'float' in both physical position and perturbational phase space. A many-parameter optimization analysis such as this presents computational difficulties. Aberrations in the primary mirror, secondary mirror and each surface of the triplet corrector lens (6 surfaces) are each defined by the coefficients of the first 36 Zernike polynomials and position in the x, y and z Chandra spacecraft body coordinate system. Furthermore, the aperture, secondary support structure, focal plane and Fiducial Transfer Mirror (which transfers light from calibration sources mounted on the Chandra X-ray optical bench to the aspect camera optical path and is responsible for the C-shape of the PSF) are each defined by a location in x, y and z as well as a rotation about the Chandra x axis. It is computationally impractical, if not impossible, to allow all of these parameters to vary with respect to each other and solve for a stable and consistent set of parameters which yields the most accurate model of the PSF. Thus we have isolated the parameters of greatest importance and have investigated that restricted subset in single dimensional perturbation analyses and limited two dimensional analyses. The aberrations tilt, astigmatism, defocus, coma and spherical aberration were all determined to be significant for our work. We have allowed the coefficients of the Zernike polynomials corresponding to these aberrations to vary in our analysis along with position and rotation.

Our most accurate raytrace PSF model built to date produces centroiding results that are more than two orders of magnitude worse than both the shift and add PSF model and the elliptical gaussian centroiding technique. The reason for the poor performance of the raytrace PSF fitting technique is not fully known at this time. It is suspected to be due to the computational difficulties of finding the true optimum optical parameter description for the ACA. Given the poor performance of the raytrace technique, the remainder of this paper will focus on the comparison of the shift and add PSF model and elliptical gaussian centroiding techniques.

2.2. The Shift and Add Method

The Shift and Add method is a technique we use to generate a super-resolved image of the ACA PSF. This is needed because the PSF has significant structure at scales smaller than the pixel size of $5''$. The basic idea is to combine many low resolution, slightly offset images into a single 'blurred' high resolution image, and then deconvolve using an appropriate kernel to recover a reasonable approximation of the true PSF. During normal science operations, the Aspect Camera focal plane is read out at 1.7 second intervals while Chandra dithers in a lissajous pattern with a period of 12 minutes and an amplitude of $8''$. Making use of the full onboard aspect solution, derived from the tracking of 5 guide stars, 3 fiducial lights and 2 gyros each reporting attitude data in 2 axes, we determine the centroid of each 1.7 second readout of the Aspect Camera. Each image is then resampled onto a 12 times subpixelated grid such that the centroid of each individual image lie in the central subpixel of the grid. Since the dither angle traveled during a 1.7 second integration is much smaller than the $5''$ ACA pixel size, shifting and stacking the individual images in this way can significantly improve the effective angular resolution of the Aspect Camera. Each output subpixel receives the total integrated counts of all 'actual' pixels stacked above it. This shifted and stacked image is then deconvolved with a kernel representing the ACA pixel size and the readout centroid distribution through the Richardson-Lucy method[3,4]. The final high resolution PSF is then normalized to unit energy (Figure 3).

Each individual image is filtered for cosmic ray hits and hot pixels before stacking it to the shift and add output grid. The shift and add PSFs are limited in spatial extent by the finite size of the guide star readout window. The dither amplitude slightly extends the spatial extent, but only to approximately $40''$ square.

Because the shape of the PSF varies significantly with changing focal plane position, we build a 13x13 grid of PSFs across the CCD at 90 pixel intervals. Since we cannot specify our input data to be collected at the grid positions we desire, we produce super-resolved PSFs at hundreds of positions across the focal plane at locations of guide stars tracked during Chandra pointings, then use a multiple surface fitting technique to build the regular super resolved PSF grid. The regular grid is *based* upon the collection of high resolution PSFs but does not *contain* any one of the super-resolved PSFs in our sample.

Each PSF in the regular super-resolved grid is 120 subpixels square. To calculate the value of each subpixel, we fit a surface in X focal plane position, Y focal plane position and intensity to the corresponding subpixels from all nearby shift and add PSFs in our library. After doing this for all 120x120 subpixels in a single grid PSF, we have 14400 surfaces and 14400 modeled subpixels. These 14400 subpixels make up one of the PSFs in the grid. We repeat this process for all 169 grid positions (Figure 4).

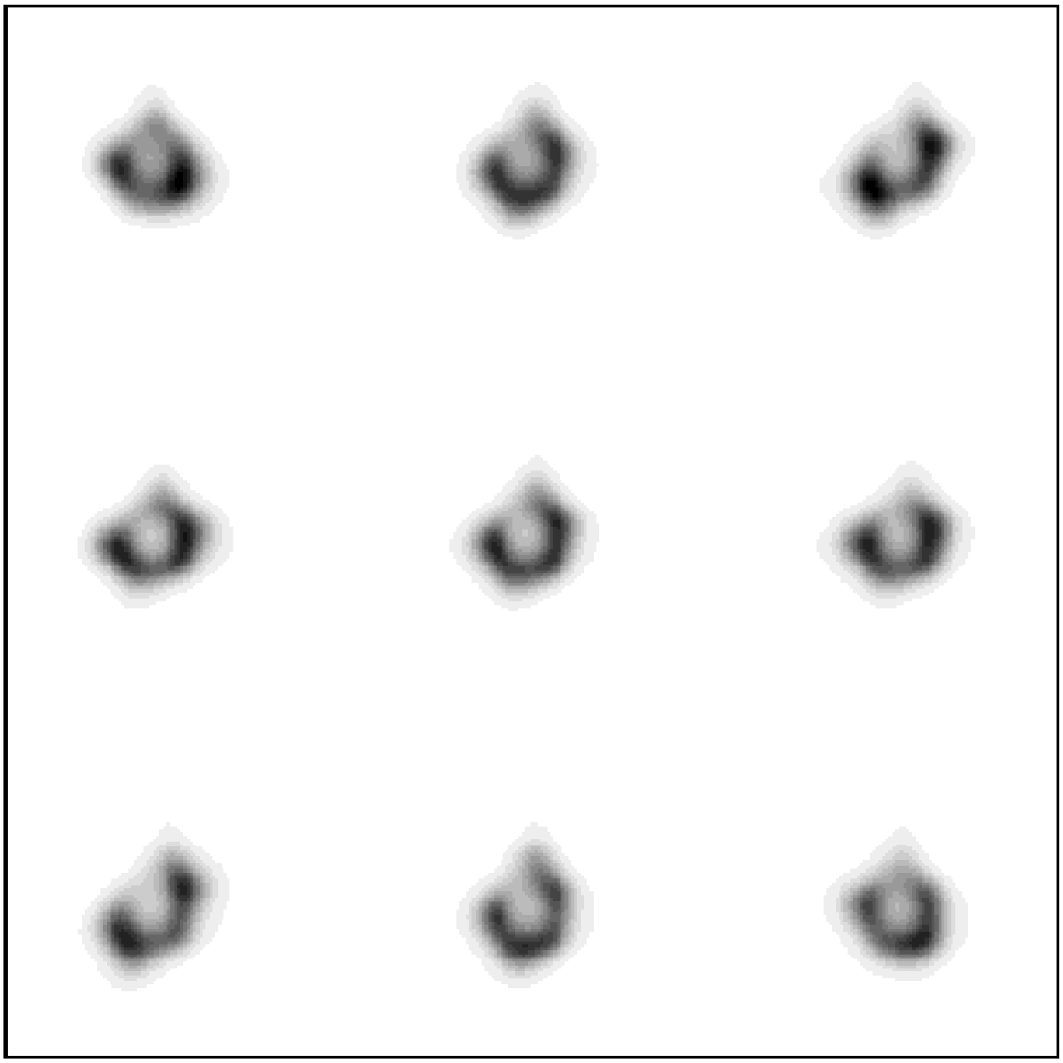

Figure 2. The (magnified) PSF images in this figure demonstrate the variation in PSF as a function of focal plane position. Each of the 9 PSFs seen in this 3x3 grid is a super-resolved shift and add PSF from our constructed library. The grid shown has x and y positions of -450, 0 and 450 in ACA pixel coordinates.

A driving force behind the accuracy of this technique is the density of data coverage which we are able to achieve over the ACA focal plane. We use a simple 2 dimensional polynomial to fit the data across the focal plane. The optical distortions of the ACA optics are much more complex than such a polynomial and thus, to improve the accuracy of the 2 dimensional polynomial approximation to the true shape of the distortion mapping, only data from a local region of the Aspect focal plane is used to build a PSF at any particular row/column position. As we shrink the radius about the PSF position from which we use data to produce our fit, we obviously shrink the amount of data to which we fit. Thus we have the amount of data available for fitting competing with the relevance of the data to the desired PSF position. With our current density of coverage (Figure 5) we have determined a data radius of $500''$ (100 ACA pixels) to produce optimal results.

3. PIPELINE RESULTS

The primary motivation behind the generation of a model of the Aspect Camera PSF is to improve the centroiding accuracy of Chandra's post facto aspect solution. Thus, to determine whether or not we have been successful, we

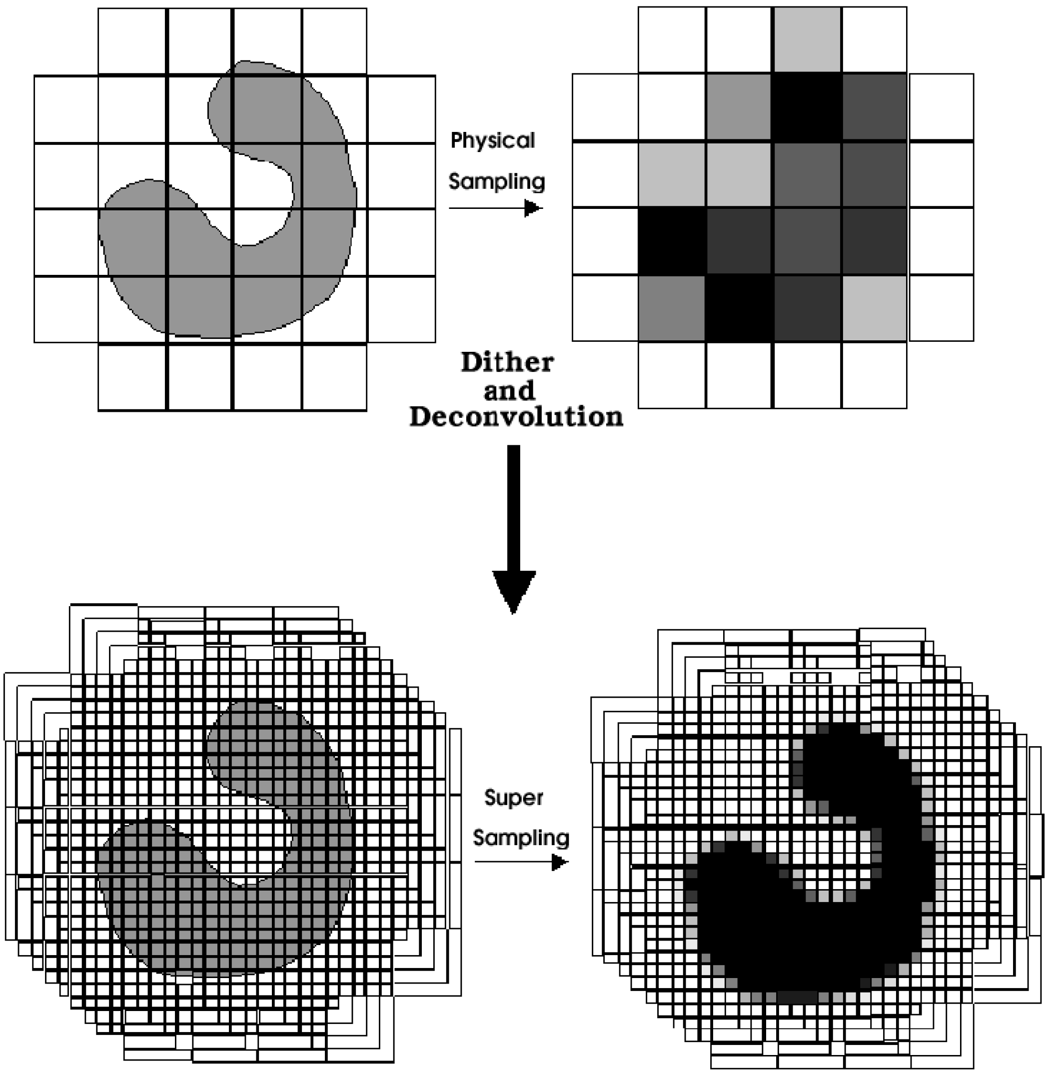

Figure 3. The true shape of the ACA PSF is coarsely sampled by the camera's native pixel size of 5″. As the telescope dithers, the image of the star moves across the focal plane at intervals of much less than a pixel between successive readouts. We use the spacecraft aspect solution to "de-dither" the images (aligning the centroids) and add them together. We then deconvolve the shifted and added image with a kernel representing the native pixel size and the distribution of centroids to produce a super-resolved composite image of the PSF.

reprocessed several Chandra science datasets through the post facto aspect processing pipeline software using both PSF fit centroiding and the standard elliptical gaussian fit centroiding, and then compared the results. We have trended our results against Aspect Camera stellar magnitude and off-axis angle to determine which part of the data space is most/least affected by the use of PSF fit centroiding.

3.1. Data Trending

Forty-seven Chandra observations have been selected from the Chandra data archive for reprocessing. We have selected observations from the very early stages of the mission (around October 1999) and also from much later in the mission (January of this year) to determine if the PSF fitting technique is sensitive to mission elapsed time.

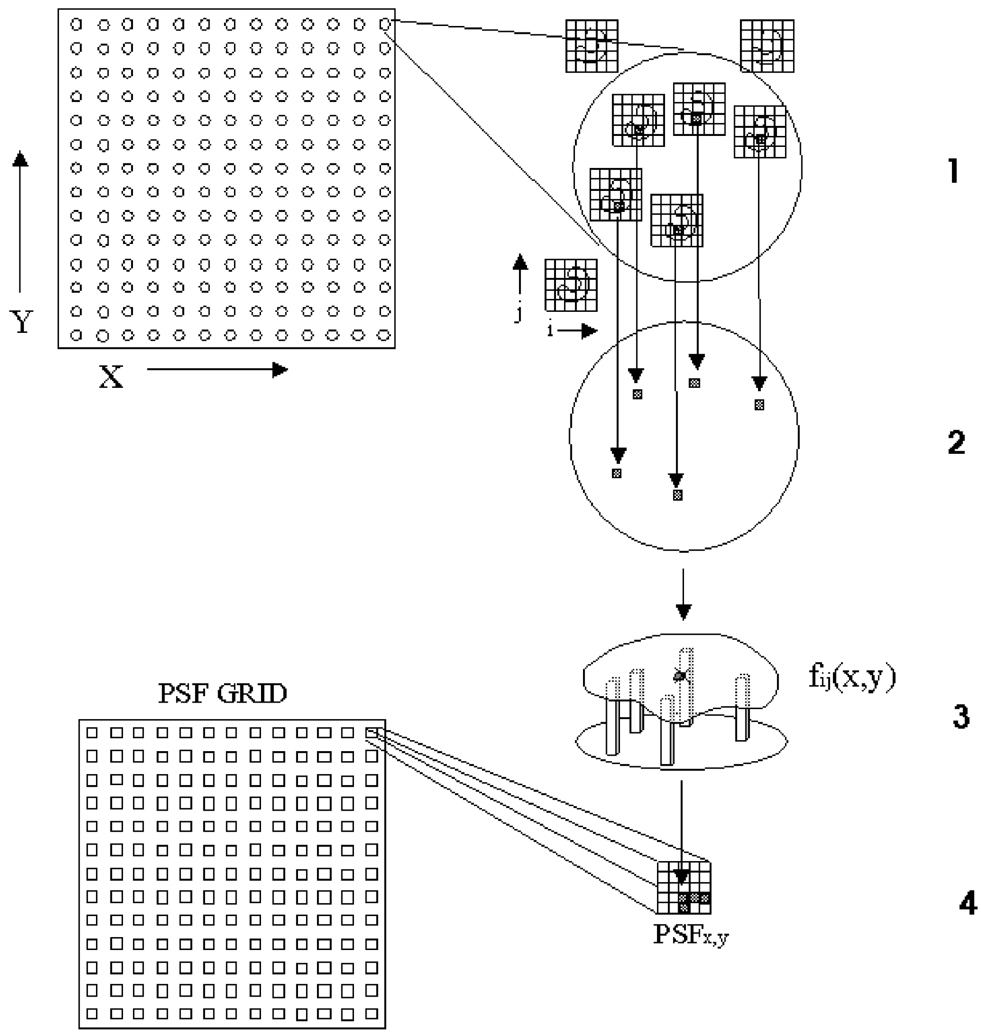

Figure 4. The aspect pipeline software uses a regular 13x13 grid of PSFs to interpolate a PSF at the focal plane position of the star it needs to centroid. The method of building this grid is shown schematically above. Step 1 - All super resolved PSFs within 500$''$ of the first grid point (x,y) are selected from the library. Step 2 - A surface, f_{ij}, is fit, subpixel by subpixel, to all selected PSFs. Step 3 - The value of the surface f_{ij} at the first regular grid point (x,y) is calculated and Step 4 - recombined to build a super resolved PSF at the first grid point. This is repeated for all points in the 13x13 grid.

Each Chandra observation nominally uses 5 stars in determining the aspect solution, though occasionally only 4 or fewer stars are used in the solution due to various reasons. Our 47 observations track 232 stars. Some statistics describing this data set are contained in Table 2 below.

Perhaps the single largest contributor to individual observation aspect uncertainty is warm or hot pixels. The Chandra Aspect Team has defined a hot pixel on the ACA focal plane to be one which has a dark current greater than or equal to 150 e^{-}/sec. Elliptical gaussian centroiding is susceptible to hot pixel induced deviations but PSF fit centroiding is believed to be less susceptible to such deviations as hot pixels are effectively deweighted in the centroid calculation. Within the 47 reprocessed observations are 21 that are known to contain hot pixels. A separate analysis

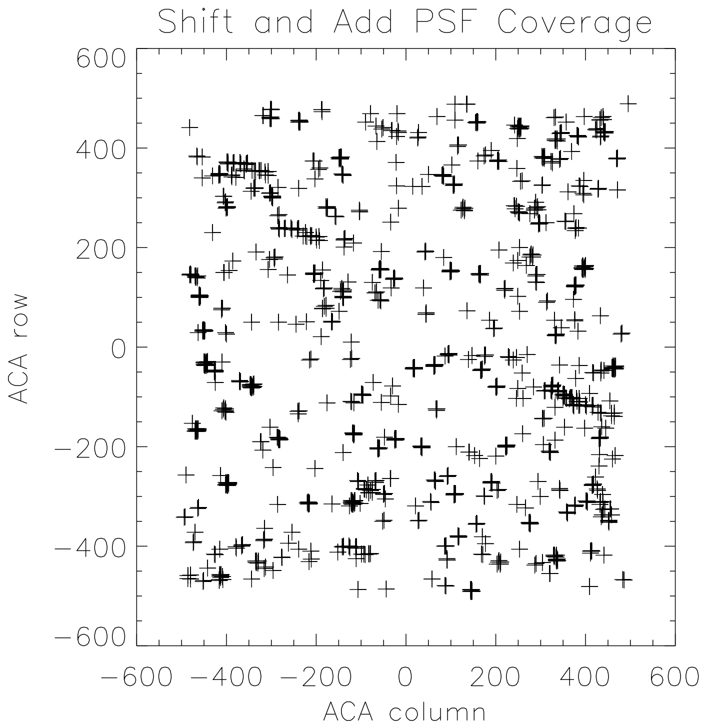

Figure 5. The coverage/density of the Shift and Add PSF library built. The full 1024x1024 pixel field of view of the ACA CCD is shown with the location of each super-resolved PSF in our library indicated by a +. The focal plane is well covered though some gaps clearly exist. Further shift and add processing to fill these gaps is planned for future work.

Table 2. Chandra Data at Large Randomly Selected Dataset

	Total	Pre-2000	Post-2000
Number of Obs	47	31	16
Number of Stars	232	153	79
Mean Magnitude	8.6	8.8	8.3
Max/Min Magnitude	11.0/6.6	11.0/6.6	10.4/7.2

of these 21 observations has not shown results significantly different from the rest of the investigated dataset. For this reason, the figures and tables in this section address the entire 47 observation dataset together.

In Figure 6 we trend the centroiding accuracies of these data against stellar magnitude, aspect camera off-axis angle and time. Figure 7 shows histograms of numbers of stars in 0.01 arcsec error bins for each centroiding technique in the 2 epochs.

Clearly, elliptical gaussian centroiding produces smaller centroiding errors than our super-resolved PSF library in practically all regions of the data set investigated. It is interesting to note that the difference is far more pronounced in the post-2000 data subset than in the pre-2000 data subset. This may indicate a real change in the ACA PSF with time due to alignment shifts or other changes in either the focal plane or the optics. This would imply that separate PSF libraries are needed to address these different data epochs.

Table 3 displays, side by side with the results of elliptical gaussian processing, the results of reprocessing this

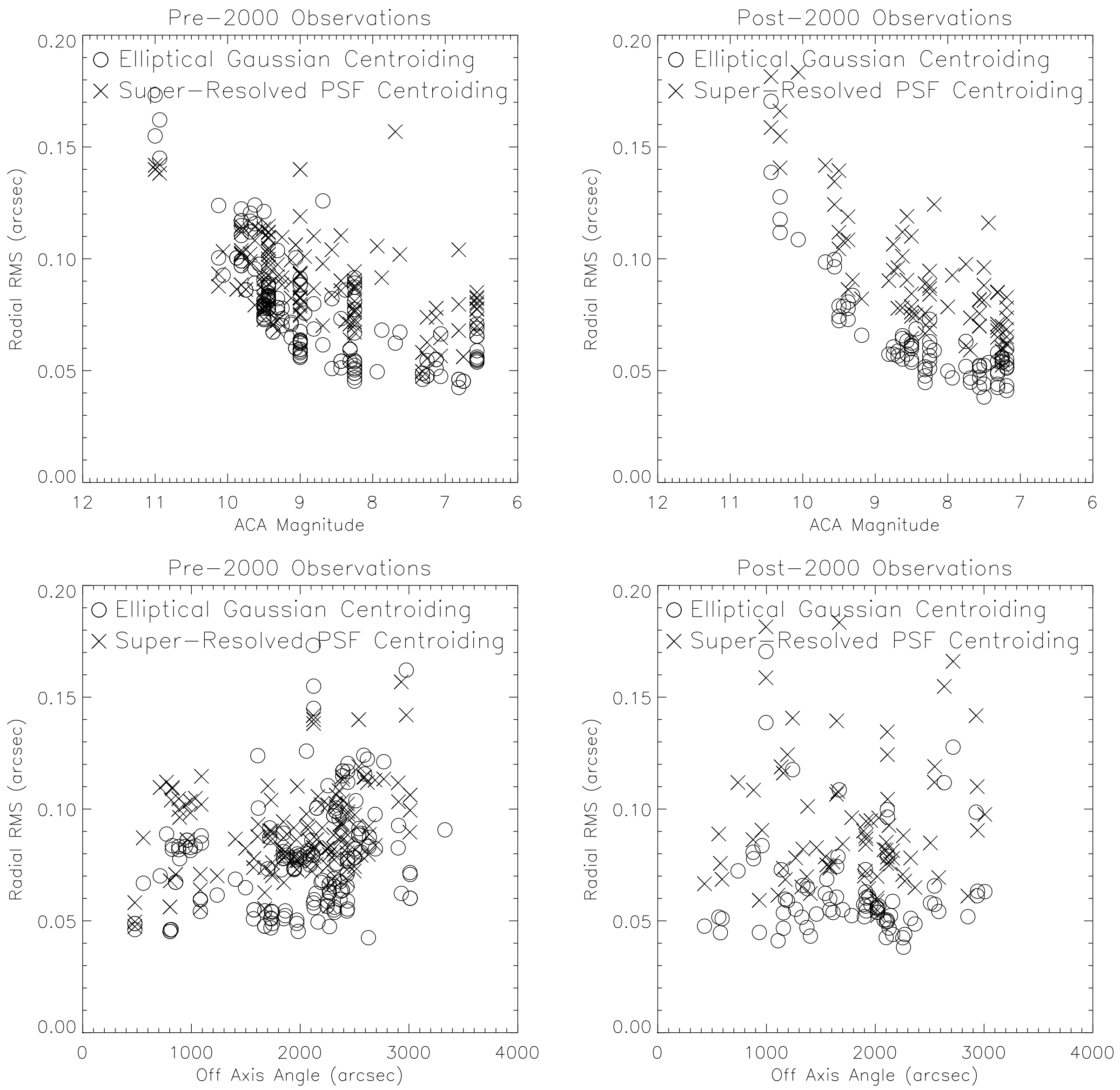

Figure 6. The upper and lower two panels in this figure show different characteristics of the same data. The upper panels show a comparison of the elliptical gaussian centroiding results to the PSF centroiding results as a function of stellar magnitude. The lower panels show the same data but as a function of aspect camera off-axis angle. In both the upper pair and the lower pair, the left panel displays data taken prior to January 1 2000 while the right panel displays data taken after January 1 of 2001 (separated by one full year).

data set using Shift and Add PSF fit centroiding. We find that the accuracy of the post-facto aspect solution of a randomly selected Chandra observation is degraded by the incorporation of PSF fit centroiding using our current ACA PSF model library.

4. CONCLUSIONS AND FUTURE WORK

We have investigated two distinct methods of building a model of the Chandra Aspect Camera PSF. The Shift and Add technique has produced the most promising results, though it does not currently represent an improvement in centroiding accuracy over the presently used elliptical gaussian centroiding technique. This is surprising since earlier analysis of simulated Aspect Camera data, in which the fitted PSF was exactly the same as that used to generate

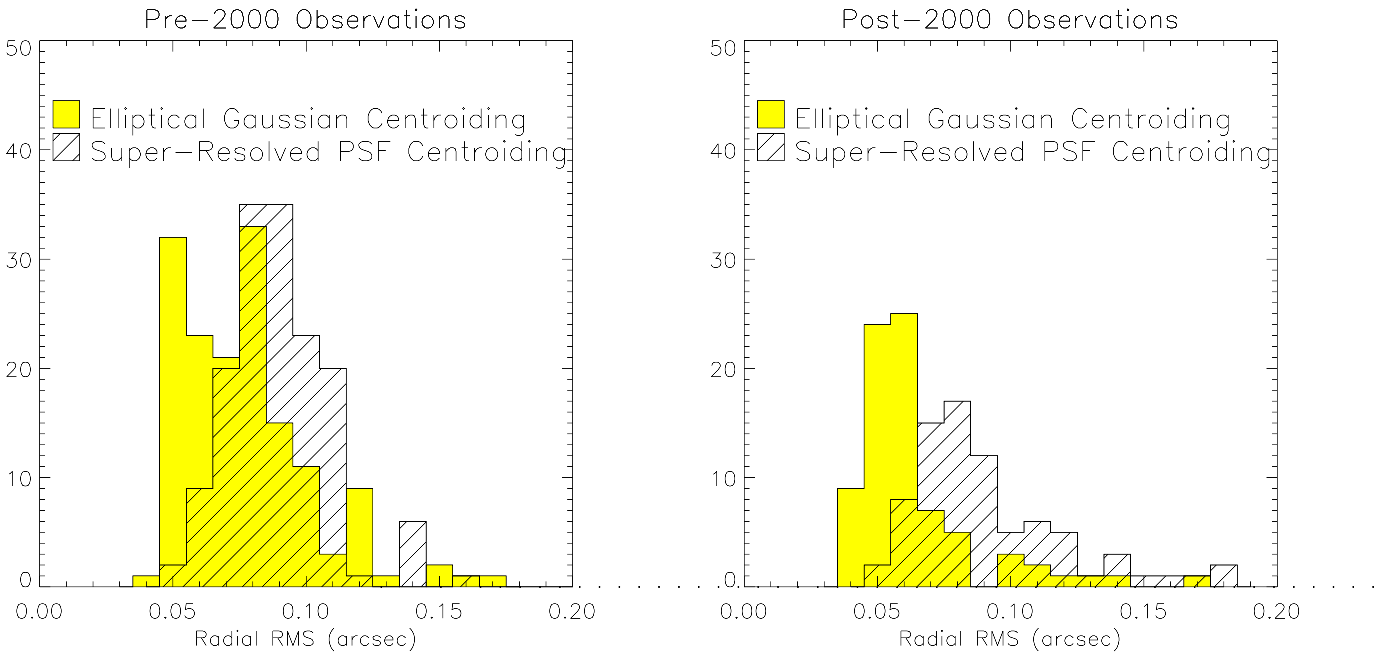

Figure 7. The left panel displays data taken prior to January 1 2000 while the right panel displays data taken after January 1 of 2001 (separated by one full year). Elliptical gaussian centroiding produces better results than PSF fit centroiding in both epochs, though the difference in performance is more pronounced in the Post-2000 data.

Table 3. Chandra Randomized Data Set RMS Centroid Error

Total	X (arcsec)	Y (arcsec)	Radial (arcsec)
Elliptical Gaussian	0.052	0.050	0.072
Shift and Add PSF	0.063	0.067	0.092
Pre-2000	X (arcsec)	Y (arcsec)	Radial (arcsec)
Elliptical Gaussian	0.055	0.053	0.076
Shift and Add PSF	0.065	0.066	0.092
Post-2000	X (arcsec)	Y (arcsec)	Radial (arcsec)
Elliptical Gaussian	0.046	0.044	0.064
Shift and Add PSF	0.058	0.070	0.091

the data, showed PSF fitting to be *more* accurate than elliptical gaussian centroiding. This would seem to imply that better fidelity is needed in the super-resolved PSF library.

As Chandra aspect data continue to accumulate, the coverage map displayed earlier becomes more and more densely filled. Constant updates to the database of available shift and add PSFs from which to draw data will improve the fidelity of the modeled PSFs. Furthermore, as the coverage density grows, we become capable of selecting data for fitting, not only on the basis of focal plane position, but also on the basis of stellar color, magnitude and time.

Finally, the shift and add technique we employ here is not wholly dissimilar to the drizzle technique employed by Fruchter and Hook[5]. While the drizzle technique has been designed mostly for use in improving the resolution of data in which there are sample sizes of a few, it is quite possible that the technique will work as well or possibly better than straight shift and add techniques on our dataset, consisting of sample sizes of a few thousand. We will investigate the use of the drizzle technique for recovery of the ACA PSF.

ACKNOWLEDGMENTS

The authors would like to thank Pete Daigneau for much initial work in developing the raytrace model of the ACA and Dave Redding for much help in understanding the MACOS and VSIM raytracing packages. Roger Hain has provided much help in developing the post-facto aspect pipeline as well as in manipulating it.

REFERENCES

1. T. Aldcroft, M. Karovska, M. Cresitello-Dittmar, R. Cameron, and M. Markevitch, "Initial performance of the aspect system on the chandra observatory: Post-facto aspect reconstruction," in *Astronomical Telescopes and Instrumentation 2000*, J. Truemper and B. Aschenbach, eds., *Proc. SPIE* **4012**, 2000.
2. R. Cameron, T. Aldcroft, W. Podgorski, M. Freeman, J. Shirer, "Initial Performance of the attitude control and aspect determination sub-systems on the Chandra Observatory," in *UV, Optical, and IR Space Telescopes and Instruments 2000*, J. Breckinridge and P. Jakobsen, eds., *Proc. SPIE* **4013**, 2000.
3. Lucy, L. B. 1974, AJ, 79, 745
4. Richardson, W. H. 1972, J.Opt.Soc.Am., 62, 55
5. A. Fruchter, R. Hook,"A novel image reconstruction method applied to deep Hubble Space Telescope Images", in *Applications of Digital Image Processing XX*, A. Tescher, eds., *Proc. SPIE* **3164**, 1997.